Electrostatic Probe Investigation of Very Low Power Arcjet VELARC in IRS and ESA-ESTEC Facilities

IEPC-2019-224

Presented at the 36th International Electric Propulsion Conference
University of Vienna, Austria
September 15-20, 2019

J. Skalden*, L. Ackermann†, P.P. Upadhyay‡, G. Herdrich§ and S. Fasoulas¶
Institute of Space Systems, University of Stuttgart, 70569 Stuttgart, Germany

Tony Schönherr‖
ESA-ESTEC (now: Enpulsion GmbH), Noordwijk, The Netherlands

and

J. Gonzalez del Amo** and D. Feili††
ESA-ESTEC, Noordwijk, The Netherlands

Plasma diagnostics using Langmuir probes are relatively simple in application, but interpretation of the data is a complex process. The results are sensitive to the vacuum quality and facility effects. The European Space Agency (ESA) and the Institute of Space Systems (IRS) conducted a joint test campaign to identify these facility effects and to elaborate standardized measurement procedures. During the test campaign at IRS, a systematic trend of electron number densities following changes in mass-specific enthalpy could be observed. Electron temperatures follow a rather erratic pattern and seem to be insensitive to specific enthalpy changes, which was partially confirmed during the experiments at ESA-ESTEC. A significant increase in ambient pressure at ESA-ESTEC most likely resulted in a probe regime change from collision free to collision affected. The data are now being used to numerical rebuild the experiments and develop a scalability tool using the IRS in-house code SAMSA.

*Research Associate, Space Transportation: Plasma Wind Tunnels and Electric Propulsion, skalden@irs.uni-stuttgart.de.
†Student Assistant, Space Transportation: Plasma Wind Tunnels and Electric Propulsion, lackermann@irs.uni-stuttgart.de.
‡Research Associate, Space Transportation: Plasma Wind Tunnels and Electric Propulsion, uparthopratim@gmail.com.
§Head Plasma Wind Tunnels and Electric Propulsion, Space Transportation, herdrich@irs.uni-stuttgart.de.
¶Head of Department, Space Transportation, fasoulas@irs.uni-stuttgart.de.
‖Research Fellow, TEC-MPE Electric Propulsion Section, schoenherr@enpulsion.com.
**Section Head, TEC-MPE Electric Propulsion Section, Jose.Gonzalez.del.Amo@esa.int.
††Electric Propulsion Engineer, TEC-MPE Electric Propulsion Section, Davar.Feili@esa.int.

Nomenclature

e = Elementary charge, C
h = Mass-specific enthalpy, J/kg
I = Current, A
Kn = Knudsen number, -
L = Length of the non-insulated probe, m
$\dot{m}$ = Mass flow rate, kg/s
m = Mass, kg
n = Number density, m^{-3}
P = Power, W
r = Probe radius, m
T = Temperature, K
U = Voltage, V
v_i = Mean ion velocity, m/s
λ_D = Debye length, m
$\lambda_{i/e}$ = Mean free path, m
Φ = Potential, V
τ_L = End-effect-parameter, -

Subscripts

e = Electron
i = Ion
LP = Langmuir probe
Th = Thruster

I. Introduction

THE satellite market is currently expected to shift from large and costly heavy satellites to low-cost, mass produced small satellites. This development stands in contrast to the complex and expensive qualification methods of electric propulsion (EP) systems. They require high-quality vacuum facilities and complex methodologies to characterize performance and plasma parameters. Furthermore, for the latter no standardized measurement procedures are available at the moment. Characterizing a plasma plume of an EP system is subject to numerous influences like vacuum quality, power supply variations, wall effects, measurement devices, etc. To get a better understanding of those facility effects, the European Space Agency (ESA) initiated several studies with the goal of a standardized test environment.[1–3]

The Institute of Space Systems (IRS) and ESA's Electric Propulsion Laboratory (EPL) setup an interlab comparison campaign with electrostatic probe experiments conducted in both facilities. In this case single electrostatic probes, which are also called Langmuir probes, were operated. Plasma diagnostics with Langmuir probes, are simple to apply, but very complex in theory and data processing. Therefore, the choice was made to use the low-power thermal arcjet VELARC (VEry Low-power ARCjet), since it is well understood and generates only a negligible magnetic field. At first, experiments measuring the electron temperature and electron number density were conducted at IRS and later repeated in the facilities of ESA-ESTEC.[4–7] During the tests at ESA-ESTEC, a significant increase in ambient pressure occurred potentially resulting in a change of the probe regime. With the IRS in-house code SAMSA, numerical rebuilding of both experimental campaigns is being processed. The aim is to characterize the influence of the pressure variation and enable scaling of the effect. This would further enhance the understanding of the probe regime in a transitional flow case for a Knudsen number range of $0.1 \leq Kn \leq 10$.

This paper presents the progress on evaluating both experimental results and discussing the probe regime in each facility. The results are compared to preliminary achievements in the numerical rebuilding endeavor.

II. Experimental Setup

In this section, the facilities of IRS and ESA-ESTEC are introduced and the equipment displayed. Furthermore, the VELARC thruster is explained and the geometry of the Langmuir probe's design process shown.

A. Vacuum Facility at IRS

The IRS features a vacuum facility seen in Fig. 1, which was optimized for lifetime test of the flight model arcjet thruster ATOS.[8] It consists of a chamber with a diameter of 1 m and 2 m length and a three-stage pumping system listed in Table 1. During operation, an ambient pressure of 0.6–0.7 Pa is provided with an argon mass flow rate of 20–30 mg/s. A water cooling system protects instruments and wiring from overheating.

Figure 1: Vacuum facility at IRS for arcjet experiments

Table 1: Vacuum facility pumps at IRS

Number	Type	Suction rate
I	Rotary vane pump	$275\,m^3/h$
II	Roots pump	$2050\,m^3/h$
III	Roots pump	$12000\,m^3/h$

B. Vacuum Facility at ESA-EPL

At ESA-ESTEC, the Langmuir experiment was setup in the EPL's SPF facility. It consists of a main chamber with 2 m diameter and a length of 4 m and a smaller hatch chamber, which is 1.2 m long at 1 m diameter. Vacuum conditions are provided by the pumps listed in Table 2. During operation of VELARC, it was found that at minimum stable mass flow rate the turbo-molecular pumps were saturated and had to be turned off. This lead to the pressure increase described in the results section.

Table 2: Pumping system of the vacuum facility at ESA-ESTEC.

Chamber	Type	Suction rate
Hatch	Scroll pump	$30\,m^3/h$
Hatch	Turbo-molecular pump	$1440\,m^3/h$ (N_2)
Main	Roots pump	$1000\,m^3/h$
Main	Screw pump	$250\,m^3/h$
Main	Primary pump	$30\,m^3/h$
Main	Turbo-molecular pump	$7320\,m^3/h$ (N_2)

C. Thermal Arcjet VELARC

Thermal arcjet thrusters have been a focus of electric propulsion development at IRS for decades. The VELARC thruster is an attempt to achieve stable operating conditions in the very low power range of 100–400 W. The model depicted in Figure 2 is a derivative of the earlier developed TALOS (Thermal Arcjet for Lunar Orbiting Satellite) thruster.[9] During several test campaigns, it was operated with hydrogen, helium, ammonia, and argon.[10]

Although argon is not a preferable propellant for electrothermal thrusters, due to the high molecular mass, it has certain advantages for this study. As monatomic gas, no energy is lost to a dissociation process, which contributes to a more stable operational behavior. Furthermore, argon does inflict negligible chemical reactions on the probe and, hence, the measurement results. Another advantage in this joint test campaign are the lower safety requirements compared to hydrogen or hydrazine, which eliminate extra effort to prepare the facilities.

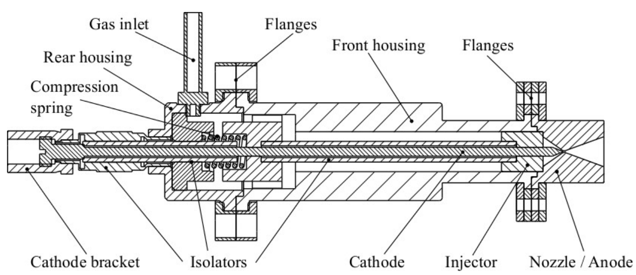

Figure 2: VELARC schematic in TALOS configuration.[11]

D. Power Supply

Power supply of the VELARC thruster is controlled with the engineering model of the power processing unit (PPU) that was originally used for the ATOS thruster.[8] Once ignition is triggered, a high-voltage pulse of up to several kilovolts is applied to cause a Paschen breakdown between the thruster's anode and cathode. Right after the arc is established, the voltage rapidly decreases to prevent damage to the electrodes and switch to steady-state mode. The adjustable current is then controlled via high-frequency voltage oscillations. The voltage and current to operate the PPU is delivered by a Delta Electronica SM 3540-D power supply, which serves as interface to the low-voltage electrical grid.

At IRS, the thruster voltage U_{Th} and current I_{Th} are measured by an in-house made multimeter. The current is derived via the voltage drop over a $100\,\Omega$ shunt.

At ESA-ESTEC, the same power supply equipment was brought there to diminish changes in the arc behavior. Here, the thruster parameters were recorded with a Yokogawa 701926 differential voltage probe and a current clamp.

E. Langmuir Probe Setup

This section introduces the Langmuir probe test setup, consisting of a 2-axis positioning system, a water cooled probe holder, and the Langmuir probe design.

1. *Langmuir Probe Design*

The design of a Langmuir probe is mostly driven by two parameters, the mean free path $\lambda_{i/e}$ and Debye length λ_D. Those determine the probe regime, which is preferred to be collision free with a thin space-charge sheath around the probe. Table 3 presents a list of conditions that need to be fulfilled to achieve the desired environment. A parameter to be introduced is the end-effect-parameter τ_L, which describes the proportion of current to the end surface of a linear probe that is positioned parallel to the plasma flow. Considering single ionized argon with an ion mass of $m_i = 6.63 \cdot 10^{-26}$ kg and a mean ion velocity of $v_i = 3000\,\mathrm{m/s}$, the end-effect parameter significantly exceeds the required $\tau_L > 50$, which means the current can be neglected during data post-processing.[12]

Table 3: Conditions to be fulfilled for a collision free, thin space-charge sheath, shown with the reference design parameters.

No.	Condition	
1	$Kn = \frac{\lambda_{i/e}}{r} = \frac{2.178\cdot10^{-4}}{1\cdot10^{-4}} = 2.178 \gg 1$	✓
2	$\lambda_{i/e} \gg r \gg \lambda_D$ $2.178 \cdot 10^{-4}\,\mathrm{m} \gg 1 \cdot 10^{-4}\,\mathrm{m} \gg 1.543 \cdot 10^{-6}\,\mathrm{m}$	✓
3	Probe positioned parallel to plasma flow	✓
4	$\frac{L}{r} = 100 \gg 1$	✓
5	$\frac{L}{\lambda_D} = 6481 \gg 1$	✓
6	$\tau_L = \frac{L}{\lambda_D} \cdot \frac{\sqrt{\frac{k \cdot T_e}{m_i}}}{v_i} = 1558 \gg 50$	✓
7	Electron/ion energy distribution has to be Maxwellian	

The two main parameters $\lambda_{i/e}$ and λ_D require knowledge of the plasma plume's electron temperature T_e and electron number density n_e. Both are to be measured in the experiments, therefore, an iterative approach is necessary by applying reference values from literature first and re-evaluate the conditions later with the actual data. The probe design depicted in Fig. 3 is the result of summarizing and averaging the measurement results from three previous experiments conducted with thermal arcjets.[13–15] Those were operated with hydrogen and secondary hydrazine, which compared to argon need to be dissociated. Since this does not apply to argon, less ionization energy is required, which was considered by reducing the averaged electron temperature by 1/3.[16]

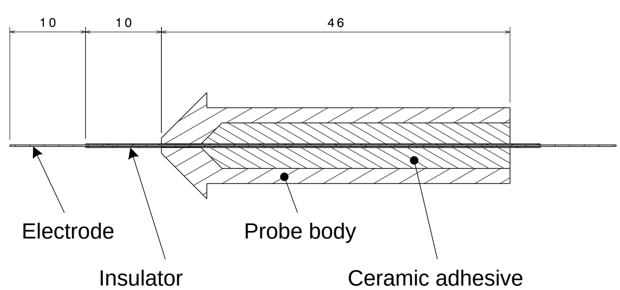

Figure 3: Schematic of the Langmuir probes used in both facilities.

To investigate systematic trends like contamination of the probe tip, a series of seven identical probes was manufactured. Five of them were operated during the IRS measurement campaign and the other two at ESA-ESTEC. The length of the non-insulated probe wire at the tip is an important parameter to derive the electron number density from the recorded current-voltage characteristics. Therefore, the manufacturing tolerance was investigated, leading to a standard deviation of $\Delta L = 0.412\,\mathrm{mm}$ between the five IRS probes. Probe 6, used at ESA-ESTEC, follows this pattern, however, Probe 7 deviated significantly more with a length of $L = 8.502\,\mathrm{mm}$.

The probes were biased by a function generator built in-house at IRS. It allows sine wave, ramp, or triangular shaped voltage biasing for frequencies in the range of 10–10,000 Hz. Differential voltage probes measure the probe potential and the probe current via a shunt. The latter can be adjusted to find an optimum between influencing the measurement and signal amplification. The sine function was selected to bias the Langmuir probes.

2. Probe Holder

A probe holder was designed over the scope of a student thesis, to mount the Langmuir probes.[16] The design criteria were simple and reliable swapping of the probes without inflicting any damage, protection of the wiring, and cooling of the probe. The latter is crucial to allow long time exposure in a thermal plasma. As seen in Figure 4, the holder features an internal cooling channel system, which is connected to a low-pressure water line. An interface plate isolates the probe holder from the tank potential to prevent grounding of the reference body.

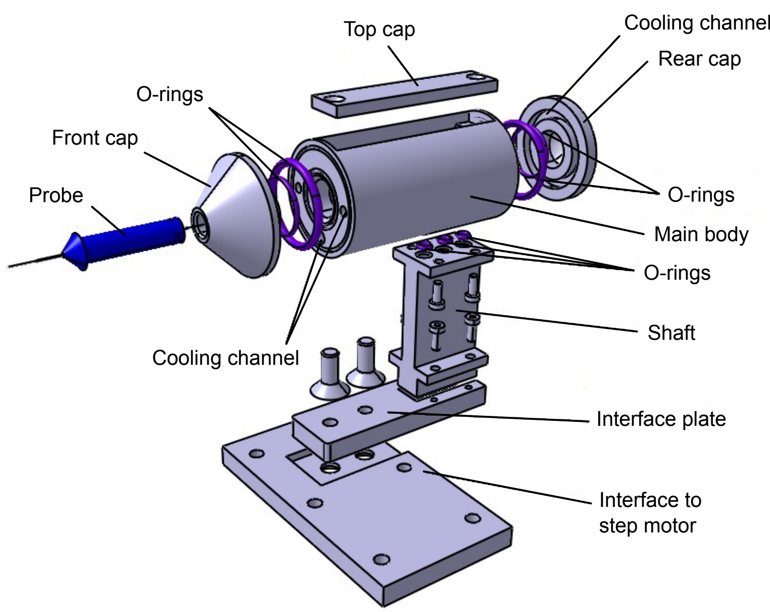

Figure 4: Exploded view of the probe holder

3. Mounting Structure

The whole Langmuir system is mounted on a 2-axis mounting structure. Two linear units attached to step motors provide precise positioning of the Langmuir probes in vacuum conditions. Heat shields made of copper with welded on copper pipes connected to the facilities water supply, keep the motors' and linear units' temperature in their operational range. This allows repositioning of the probe during thruster operation to record axial and radial profiles of the plasma plume.

F. Test Matrix and Procedure

During preparation of the VELARC thruster for the IRS experiments, a stable operation point was found at $I_{Th} = 9\,\mathrm{A}$ and $U_{Th} = 16\,\mathrm{V}$ at the minimum argon mass flow rate of $\dot{m} = 17\,\mathrm{mg/s}$.[4] Due to the operational principle, the voltage slightly oscillates to keep the current stable. These were set as standard conditions at both facilities.

Before conducting the Langmuir probe measurements, the thruster was operated for about 1 hour to reach thermal equilibrium of the nozzle material. The long time frame can be explained by the wall thickness of the nozzle. Since it was derived from TALOS, which was designed for higher power levels, the heating time needs to be longer for low-power applications. This procedure however, is crucial to reach the aforementioned stable operating conditions.

The recorded Langmuir probe measurands were the probe potential Φ_{LP} and probe current I_{LP}. In both facilities, the controlled parameters were the distance between nozzle exit plane and probe tip d starting at 60 mm with an increment of 10 mm and the probes themselves. Furthermore, at IRS each probe was tested five times to investigate contamination and heating effects. This was not possible at ESA-ESTEC, due to the limited time frame.

Table 4: Test matrix for the test campaigns with different probes.

Probe	$\dot{m}$	I_{Th}	Φ_{LP}	Measurands
Probe 1	17 mg/s	9 A	-10–+15 V	Φ_{LP}, U_{Th}, I_{LP},I_{Th}, $\dot{m}$
Probe 2	17 mg/s	9 A	-10–+15 V	Φ_{LP}, U_{Th}, I_{LP},I_{Th}, $\dot{m}$
Probe 3	17 mg/s	9 A	-10–+15 V	Φ_{LP}, U_{Th}, I_{LP},I_{Th}, $\dot{m}$
Probe 4	17 mg/s	9 A	-10–+15 V	Φ_{LP}, U_{Th}, I_{LP},I_{Th}, $\dot{m}$
Probe 5	17 mg/s	9 A	-10–+15 V	Φ_{LP}, U_{Th}, I_{LP},I_{Th}, $\dot{m}$
Probe 6	17 mg/s	9 A	-10–+15 V	Φ_{LP}, U_{Th}, I_{LP},I_{Th}, $\dot{m}$
Probe 7	17 mg/s	9 A	-10–+15 V	Φ_{LP}, U_{Th}, I_{LP},I_{Th}, $\dot{m}$

III. SAMSA

Self and Applied field Magnetoplasmadynamic thruster algorithm (SAMSA) is a numerical code for investigations of basic plasma processes in Magneto-hydrodynamic (MHD) relevant plasma. It models the plasma flow as a two-phase continuum model consisting of heavy particles and electrons, while treating them both as ideal gas. This code is an in-house code under development at IRS further enhancing its capabilities. The code is currently being used to simulate rotational symmetric magneto hydrodynamic problems and arcjet thrusters for numerical rebuilding of experimental test cases.

Based on an axisymmetric finite volume method on unstructured, adaptive meshes and under the assumptions of continuum flow, condition of quasi-neutral plasma flow is modeled as a two-fluid plasma consisting of heavy particles (neutral and ionized argon) and electrons. These include Navier-Stokes equations from classical fluid dynamics for modeling heavy particles and conservation equations for the magnetic field and electron energy. Inviscid parts of the partial differential equations are solved by an upwind-scheme with flux-vector splitting, whereas viscous parts are solved by a centralized scheme. To create a spatial discretization of second order, a WENO-scheme (Weighted Essentially Non-Oscillatory) was used. It is able to simulate argon, xenon, and helium with different ionization levels and was also adapted to incorporate applied magnetic fields by using a vector-potential formulation with coils.[17]

IV. Results

In this section the results from the experiments at IRS and ESA-ESTEC are displayed and discussed in combination with the numerical results. Furthermore, the probe regime in both facilities is being discussed, due to a significant pressure difference.

A. Test Campaign at IRS

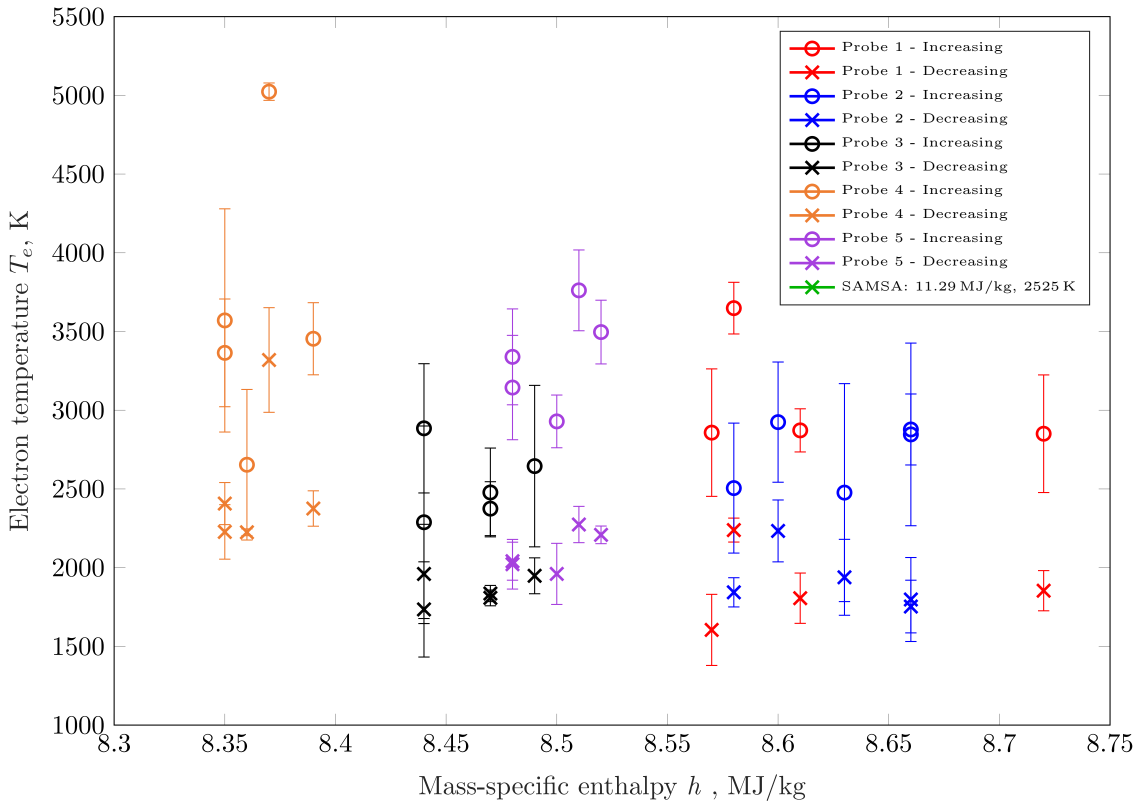

Figure 5: Electron temperature against specific enthalpy from the IRS experiments. Error bars indicate standard deviations from three measurements (Based on Ref. 4). For the sake of better visibility, the numerical results are displayed in the legend.

The electron temperature and number density results from the IRS campaign are displayed in Fig. 5 and Fig. 6. In both diagrams, the data are plotted against the mass-specific enthalpy of the VELARC thruster, which is the applied power divided by the mass flow rate. The mass specific-enthalpy serves as parameter to evaluate the reproducibility and indicate potential facility effects. As it can be seen, a range of about 8–9 MJ/kg is covered, which is caused mainly by voltage adjustments to keep the thruster current level stable. Another contribution comes from small deviations of the mass flow controller, however their influence is comparably small.

The electron temperatures and number densities are separated into increasing and decreasing voltage sweeps of the applied sine function bias. The reason lies in an observed hysteresis effect, which was likely caused by heating of the probe. Contamination can be rather ruled out, since the hysteresis remained constant over the scope of five measurements per probe.[18] This lead to a slightly higher range of electron temperature measurements for increasing voltage sweeps of 2300–3700 K compared to 1700–3400 K from decreasing sweeps. However, most of the difference between the voltage sweeps lies within the measurement uncertainty, here displayed as standard deviation of three measurements. In general, the electron temperatures seem to be rather insensitive towards mass-specific enthalpy variations, as their behavior is apparently not following a systematic trend.

The reference studies used for designing the probe show electron temperatures in the same order of magnitude, however at significantly higher mass-specific enthalpies ranging from 22.4–73.3 MJ/kg.[13–15] This can be explained with the difference in used propellants. Burton and Habiger operated the arcjet with secondary hydrazine and Gallimore with hydrogen. Since VELARC was operated with argon, the required ionization energy was lower, hence, requiring a lower mass-specific enthalpy.

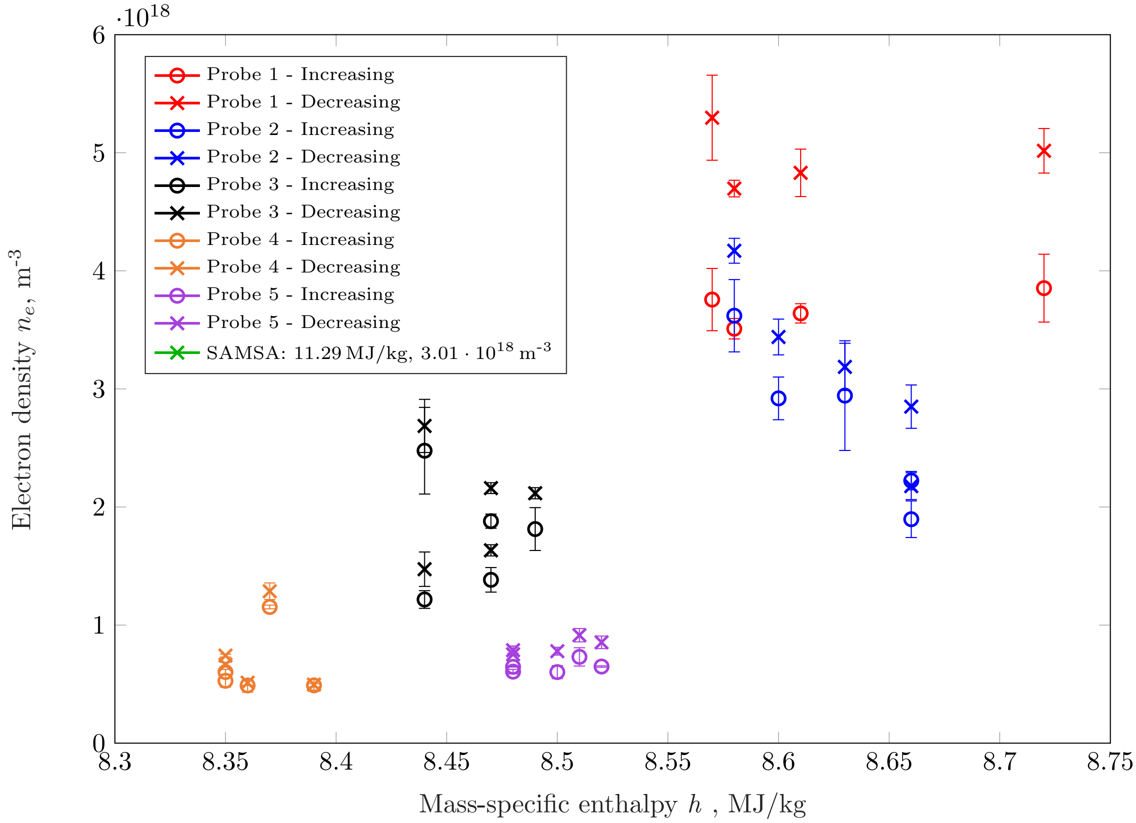

Figure 6: Electron densities against specific enthalpy from the IRS experiments. Error bars indicate standard deviations from three measurements (Based on Ref. 4). For the sake of better visibility, the numerical results are displayed in the legend.

The electron number density data show a different behavior than electron temperatures. The hysteresis effect causes the exact opposite, with increasing voltage sweeps showing a lower range between 10^{18}–$3.8 \cdot 10^{18}$ m^{-3}, whereas decreasing sweeps reach slightly higher values ranging from 10^{18}–$5 \cdot 10^{18}$ m^{-3}. However, the order of magnitude remains the same and the differences between the sweeps are less distinct compared to the electron temperature results. More important is the fact that a clear systematic trend between mass-specific enthalpy and electron number density is present. It exceeds the measurement uncertainty, which is again described by the standard deviation of three measurements.

In comparison with the reference studies, the whole electron density range is lower, which can be explained by the different propellants used in the experiments and the above stated difference in mass-specific enthalpies.

The simulation of the IRS measurement campaign shows electron temperatures and number densities that match the average experimental results. However, the mass-specific enthalpy is significantly larger. Since mass flow rate and discharge current are boundary conditions, the remaining variable is the discharge voltage, which is indeed 2–3 V higher than during the experiments. It is assumed that the reason for this lies within the electrical conductivity of the plasma in the discharge chamber. Fine tuning of the parameter and the electrode fall region is ongoing and might result in a better matching with the thruster's operational parameters.

B. Test Campaign at ESA-ESTEC

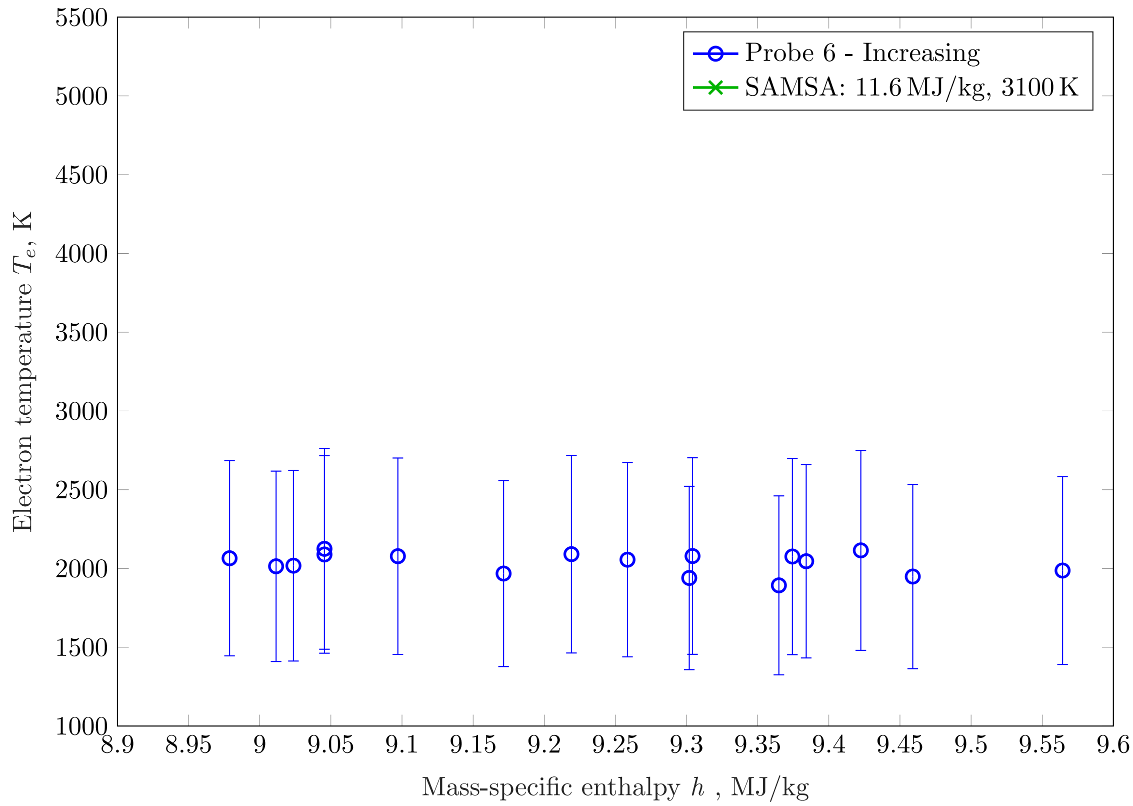

Figure 7: Electron temperature against mass-specific enthalpy for Probe 6 at ESA-ESTEC. Error bars indicate a conservatively estimated uncertainty of 30 %. For the sake of better visibility, the numerical results are displayed in the legend.

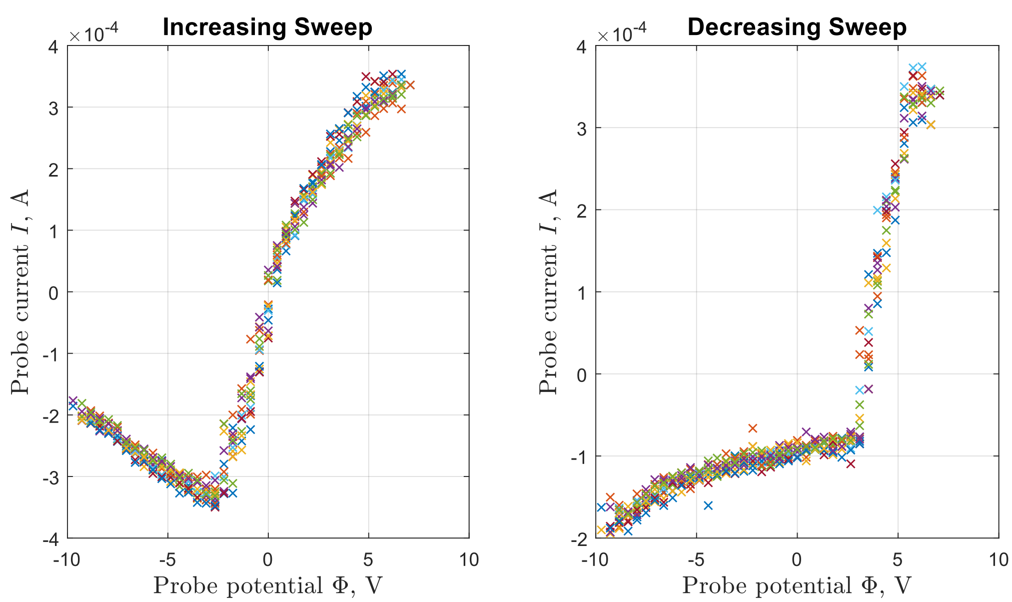

Figure 8: Current-voltage characteristics for increasing and decreasing voltage sweeps at 70 Pa

During the experiments at ESA-ESTEC, a significant increase in ambient pressure occurred, due to saturation of the turbo-molecular pumps, which needed to be shutdown to prevent damage. The vacuum system is designed mainly for electrostatic propulsion systems with low mass flow rate, which explains the cause of events. The pressure leveled out at 70 Pa during steady-state operation of the VELARC thruster. This environment had a significant impact on the recorded current-voltage characteristics, which is shown in Fig. 8. The trend line follows an abnormal behavior, which is especially visible for the increasing sweep. In the negative probe current zone, the current drops with increasing probe potential, before following a steep increase. This leads to the assumption of artifactual behavior of electrons. Another problem is that neither ion nor electron saturation is reached, which is likely due to the pressure increase and, hence, insufficient maximum probe potential. As a result, electron number density cannot be derived from this characteristic assuming a collision free, thin plasma sheath. Only the electron temperature for the increasing sweep could be derived under these assumptions, displayed in Fig. 7. However, the probe regime is not clear and is further discussed in the next section, so the results must be treated with caution.

The results for increased voltage sweeps are at the lower edge of the electron temperature range measured at IRS. The uncertainty displayed is at the moment a conservatively estimated 30 % of the reading, which is standard for Langmuir probe results. Compared to IRS, the results are less erratic and stay rather constant at about 2000 K, but are significantly wider spread over the mass-specific enthalpy. At IRS, a single probe covers a range of about 0.05 MJ/kg, whereas at ESA-ESTEC it is about 0.6 MJ/kg. Also the range itself is higher with 8.98–9.56 MJ/kg compared to the one at IRS with 8.35–8.73 MJ/kg. This can be explained by a fault in the ATOS PPU, which applied 10 A instead of 9 A to the thruster.

The numerical result is slightly above the measured electron temperature range. Considering the currently limited data points and the fact that only the results of one probe could be processed so far, this might turn out to match the final data set. The mass-specific enthalpy is again significantly larger than the experimental result, but the difference between the simulations and the facilities is in a similar range. This supports the theory that the electrical conductivity is not set to the correct value yet. The electron density results to $3.03 \cdot 10^{16}\,\mathrm{m^{-3}}$, which is exactly two orders of magnitude below the average results at IRS. This might directly correlate to the pressure difference between the facilities.

C. Probe regime discussion

As described above in the probe design section, the probe regime has to be confirmed with the actual data. The Debye length and mean free path were recalculated by averaging the derived electron temperature $\overline{T_e} = 2556\,\mathrm{K}$ and electron number density $\overline{n_e} = 2.024 \cdot 10^{18}\,\mathrm{m^{-3}}$ from the IRS measurement campaign. In Table 5 the conditions for a collision free, thin space-charge sheath regime are checked again.

Table 5: Conditions to be fulfilled for a collision free, thin space-charge sheath, revised with measured parameters.[19]

No.	Condition	
1	$Kn = \frac{\lambda_{i/e,new}}{r} = \frac{5.234 \cdot 10^{-4}}{1 \cdot 10^{-4}} = 5.234 \gg 1$	✓
2	$\lambda_{i/e,new} \gg r \gg \lambda_{D,new}$ $5.234 \cdot 10^{-4}\,\mathrm{m} \gg 1 \cdot 10^{-4}\,\mathrm{m} \gg 2.452 \cdot 10^{-6}\,\mathrm{m}$	✓
3	Probe positioned parallel to plasma flow	✓
4	$\frac{L}{r} = 100 \gg 1$	✓
5	$\frac{L}{\lambda_{D,new}} = 4078 \gg 1$	✓
6	$\tau_L = \frac{L}{\lambda_{D,new}} \cdot \frac{\sqrt{\frac{k \cdot T_e}{m_i}}}{v_i} = 991 \gg 50$	✓
7	Electron/ion energy distribution has to be Maxwellian	✓

With the probe characteristics recorded, the requirement for a Maxwellian energy distribution can now be assessed as well. In Fig. 9a, the exponential part of the current-voltage characteristic shows a linear gradient in the semi-logarithmic plot, which is a sign for the electrons to be Maxwellian.[20]

To determine the probe regime of the results in a pressure environment of 70 Pa, a comparison between the Knudsen numbers was made. In Fig. 9b the Knudsen number is plotted against electron temperature for the two pressure cases. These are calculated for a thermal plasma consisting of argon with a degree of ionization of 10 %, which is likely for a thermal arcjet thruster.

For the expected temperature range of up to 5000 K, the Knudsen number does not even exceed $Kn = 1$. This is clearly in the transitional flow regime, which is defined in the range $0.1 \gg Kn \gg 10$. That means the measurements obtained at ESA-ESTEC cannot be considered only collision free, but are also collision affected.

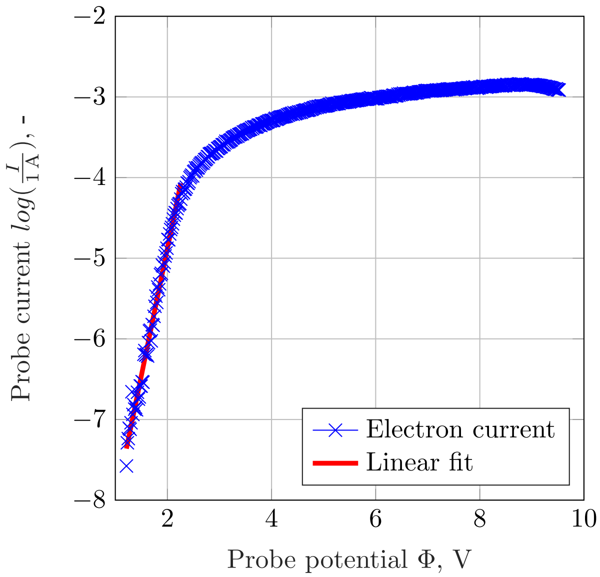

(a)

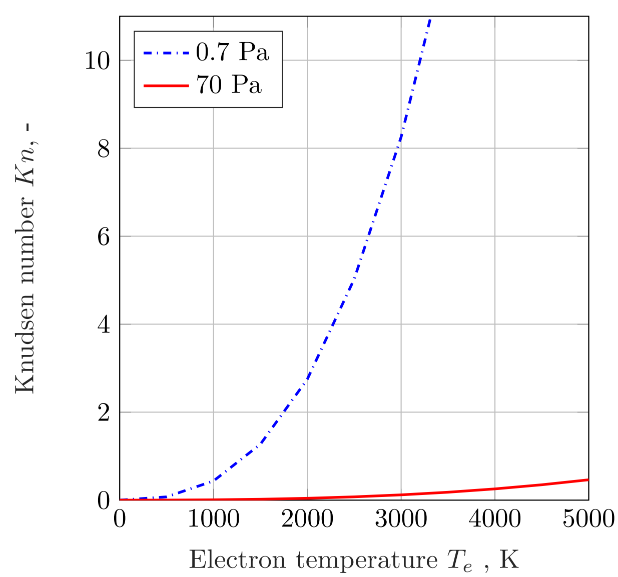

(b)

Figure 9: a) Exemplary semi-logarithmically plotted current-voltage characteristic recorded during the test campaign at IRS, b) Knudsen number against electron temperature for 0.7 Pa and 70 Pa

V. Conclusion

A Langmuir test setup was successfully operated at the facilities of the Institute of Space Systems and ESA-ESTEC. The very low-power thermal arcjet VELARC was also successfully commissioned and reached stable operation in both facilities. Furthermore, numerical simulations of both test environments were conducted. The results from the experimental campaign at IRS show a systematic behavior of electron number density measurements following changes in mass-specific enthalpy. Electron density results at ESA-ESTEC could not be derived yet to confirm this behavior. The electron temperature results at IRS seem rather insensitive to mass-specific enthalpy changes, which needs to be confirmed by the ESA-ESTEC results. Due to a significant pressure difference, the probe regime during the ESA-ESTEC campaign cannot be considered collision free. Processing of the data is still ongoing, with consideration of the probe regime change. The numerical simulation results with the IRS in-house code SAMSA match with the electron temperatures and number densities well, but with a significantly higher mass-specific enthalpy. It is assumed that further accuracy can be achieved by fine tuning the electrical conductivity in the discharge chamber plasma.

Acknowledgments

The support of the IRAS project as well as the Ministry of Economic Affairs Baden-Württemberg is greatly acknowledged.

References

[1]Blott, R. and Gonzalez del Amo, J., "European Electric Propulsion Procedures Assessment and Harmonization Study," Final Report ESTEC Contract Number 20817/07/NL/PA, January 2008.

[2]Blott, R. and Gonzalez del Amo, J., "European Electric Propulsion Verification Procedures Development Study," Final Report ESTEC Contract Number 21662/08/NL/PA, February 2012.

[3]Blott, R. and Gonzalez del Amo, J., "European Electric Propulsion Verification Procedures Development Harmonization Study," Final Report ESTEC Purchase Order N. 5401000591, February 2012.

[4]Herdrich, G., Gäßler, B., Le, Q. H., and Syring, C., "Langmuir Probe Measurements at IRS," Tech. Rep. RP-4000107273/12/NL/PA-D3b, Institute of Space Systems, University of Stuttgart, March 2017.

[5]Skalden, J., Herdrich, G., and Ackermann, L., "Comparison of Langmuir Probe Measurements at IRS and ESA-ESTEC," Tech. Rep. RP-4000107273/12/NL/PA-D4, Institute of Space Systems, University of Stuttgart, December 2018.

[6]Gonzalez del Amo, J. and Bulit, A., "ESA Propulsion Laboratory (EPL)," *IEPC-2011-004*, 32nd International Electric Propulsion Conference, Wiesbaden, Germany, September 2011.

[7]Skalden, J., Upadhyay, P. P., Ackermann, L., Herdrich, G., Schönherr, T., Gonzalez del Amo, J., Feili, D., and Fasoulas, S., "Investigation of Facility Effects with Electrostatic Probes on Thermal Arcjets," 32st International Symposium on Space Technology and Science, Fukui, Japan, June 2019.

[8]Riehle, M., "ATOS - Arcjet Flugexperiment auf dem Amateurfunksatelliten AMSAT-P3-D," Tech. Rep. Final report, DARA FKZ TT 50 TT 9404, 1994.

[9]Bock, D., *Untersuchung eines thermischen Lichtbogentriebwerksystems für die Lunar Mission BW1*, Ph.D. Dissertation, University of Stuttgart, Stuttgart, Germany, 2009.

[10]Wollenhaupt, B., Le, Q. H., and Herdrich, G., "Overview of Thermal Arcjet Thruster development," *Aircraft Engineering and Aerospace Technology*, Vol. 90, No. 2, 2018, pp. 280–301.

[11]Herdrich, G., Binder, T., Boxberger, A., Chadwick, A., Chan, Y.-A., Ehresmann, M., Harmansa, N., Montag, C., Romano, F., Skalden, J., and Fasoulas, S., "Research and Development on Electric and Advanced Propulsion at IRS," *IEPC-2017-480*, 35th International Electric Propulsion Conference, Atlanta, USA, October 2017.

[12]Herdrich, G. and Syring, C., "Electrostatic Probes: Theory and Application," Tech. Rep. RP-4000107273/12/NL/PA-D1, Institute of Space Systems, University of Stuttgart, January 2014.

[13]Habiger, H. A., Auweter-Kurtz, M., and Kurtz, H., "Electrostatic Probes for the Investigation of Arc-Driven Electric Propulsion Devices," *IEPC-93-124*, 23rd International Electric Propulsion Conference, Seattle, WA, USA, 1993.

[14]Gallimore, A. D., Kim, S.-W., Foster, J. E., King, L. B., and Gulczinski, I. F. S., "Near- and Far-Field Plume Studies of a One-Kilowatt Arcjet," *Journal of Propulsion and Power*, Vol. 12, No. 1, 1996, pp. 105–111.

[15]Burton, R. L. and Bufton, S. A., "Exit-Plane Electrostatic Probe Measurements of a Low-Power Arcjet," *Journal of Propulsion and Power*, Vol. 12, No. 6, 1996, pp. 1099–1106.

[16]Gäßler, B., *Aufbau und Inbetriebnahme einer elektrostatischen Sonde zur Charakterisierung des Abgasstrahls eines Arcjets*, Bachelor thesis, Institute of Space Systems, University of Stuttgart, July 2015, (in German).

[17]Upadhyay, P. P., Tietz, R., and Herdrich, G., "Numerical Simulation Accompanied with Shock stand-off prediction for heat-flux mitigation by MHD flow control on Re-entry Vehicles," 31st International Symposium on Space Technology and Science, Matsuyama-Ehime, Japan, June 2017.

[18]Herdrich, G., Ackermann, L., Syring, C., Le, Q. H., Skalden, J., Fasoulas, S., Schönherr, T., Feili, D., and Dannenmayer, K., "Standardized Approach for Langmuir Probe Measurements using the Low Power Arcjet VELARC," *Frontier of Applied Plasma Technology*, Vol. 11, No. 2, 2018, pp. 54–60.

[19]Skalden, J., Le, Q. H., Herdrich, G., and Fasoulas, S., "Standardization Approach on Langmuir Probe Measurements with Thermal Arcjet VELARC," *SP2018 00507*, Space Propulsion 2018, Seville, Spain, May 2018.

[20]Hershkowitz, N., "How Langmuir Probes Work," *Plasma Diagnostics*, edited by O. Auciello and D. L. Flamm, Academic Press, Inc., London, 1989, pp. 113–183.